ELSEVIER

Kinetic analysis using square-wave stimulation in modulation excitation spectroscopy: Mixing property of a flow-through PM-IRRAS cell

Atsushi Urakawa [a], Thomas Bürgi [b,*], Alfons Baiker [a,*]

[a] *Department of Chemistry and Applied Biosciences, ETH Zürich, CH-8093 Zürich, Switzerland*
[b] *Institut de Chimie, Faculté des Sciences, Université de Neuchâtel, Rue Emile-Argand 11, CH-2007 Neuchâtel, Switzerland*

Abstract

Square-wave stimulation used in modulation excitation spectroscopy [D. Baurecht, U.P. Fringeli, Rev. Sci. Instrum. 72 (2001) 3782] can have significant advantages over a simple sinusoidal-wave due to the high odd-frequency terms contained in square-wave, particularly when a system response is close to linear. Phase-sensitive detection (PSD) affords separating the signals of the different frequency terms with a high signal-to-noise ratio by averaging a number of modulation cycles. A modulation excitation experiment applying square-wave stimulation provides the same information as several experiments applying sinusoidal-wave stimulations at the same frequency as the square-wave stimulation and at higher frequencies. The amplitude and the phase lag of a response obtained by PSD at fundamental and higher frequencies using square-wave stimulation are related to the ones obtained by sinusoidal-wave stimulation using transfer function of a general system. Mixing property of a PM-IRRAS (polarization–modulation infrared reflection–absorption spectroscopy) flow-through cell was studied by a simple mixing tank model using square-wave concentration stimulation. The advantages of square-wave stimulation are shown by the characterization of the mixing property.
© 2005 Elsevier B.V. All rights reserved.

Keywords: Frequency response; Bode diagram; Transfer function; Mixing tank; PM-IRRAS; Modulation excitation spectroscopy

1. Introduction

Modulation spectroscopy, alternatively called modulation (or modulated) excitation spectroscopy (MES), is a powerful technique to investigate the dynamic behavior of chemical and physical systems [1,2]. When a system is perturbed by a periodic change of a parameter (so-called stimulation), for example concentration, pH, light flux, and temperature, affecting a chemical or physical state of the system, the response of the state will also be periodic. The periodically alternating response can sensitively be detected and the signal-to-noise ratio can be significantly enhanced by a phase-sensitive detection (PSD) [1]. PSD affords accurate determination of frequency-dependent amplitude and phase lag of responses. Also, with a broad-band analytical method, such as Fourier transform infrared spectroscopy, the separation of overlapping bands of different kinetic behavior is possible [2,3], analogous to the 2D technique applying correlation functions [4]. The practical advantages and power has led to a wide range of applications of MES, for example in heterogeneous catalysis [3], biological systems [2,5], chiral recognition [6–8], and diffusion [9].

Two kinds of stimulation are typically used in MES; sinusoidal- and square-wave stimulations. Sinusoidal-wave stimulation is simpler to treat theoretically for the quantitative analysis of the responses including the overtones. On the other hand, square-wave stimulation is often easier to generate experimentally, in particular in the case of concentration stimulation, which is generated by switching between two flows of different concentrations. PSD can

---
* Corresponding authors. Tel.: +41 44 632 31 53; fax: +41 44 632 11 63 (A. Baiker), Tel.: +41 32 718 24 12; fax: +41 32 718 25 11 (T. Bürgi).

E-mail addresses: baiker@chem.ethz.ch (A. Baiker), thomas.burgi@unine.ch (T. Bürgi).

be straightforwardly applied to analyze responses to square-wave stimulation and the benefits of MES remains due to the large fundamental frequency component of a square-wave. However, the analysis of the responses to a square-wave stimulation is more cumbersome when it comes to quantitative analysis. In this study, the relationship between responses to sinusoidal- and square-wave stimulations within a linear response assumption and practical advantages of square-wave stimulation are shown. Transfer function, derived from a linear or a linearized non-linear model, often used in signal processing, control and communication theory, and a powerful tool in frequency response analysis, is used to show the relationship between square-wave and sinusoidal stimulation and the advantages of the former are discussed. The validity and the usage of the theory are demonstrated by investigating the mixing behavior in a flow-through PM-IRRAS (polarization–modulation infrared reflection–absorption spectroscopy) cell, which was specially designed for the application of MES in PM-IRRAS [10].

2. Theory

2.1. Modulation excitation spectroscopy and phase-sensitive detection

If a system is perturbed by varying an external parameter (e.g., temperature, concentration, light flux, pH, and electric current) periodically, all the parameters in the system, which are affected by this perturbation, will also change periodically at the same frequency as the stimulation (ω) or harmonics thereof ($2\omega, 3\omega, \ldots$). The response of the affected parameters typically shows a frequency-dependent amplitude and a phase delay with respect to the stimulation. During the first periodic perturbation cycles, the affected parameters relax to new quasi-steady-state values around which they oscillate. When the response of the periodically oscillating parameter is denoted as $A(t)$, the phase-domain response at the fundamental ($k = 1$, in this work, k is called demodulation index) and harmonic ($k = 2, 3, \ldots$) frequencies are obtained by PSD (phase-sensitive detection), or so-called demodulation, according to the following equation [1]:

$$A_k(\phi_k^{PSD}) = \frac{2}{T} \int_0^T A(t) \cdot \sin(k\omega t + \phi_k^{PSD}) \, dt \tag{1}$$

PSD allows selective extraction of the $k\omega$ component of the response, thereby often used in noise reduction by removing noise at frequencies different from $k\omega$. The $k\omega$ component amplitude of a response can be accurately determined by PSD, and furthermore the in-phase angle value of ϕ_k^{PSD}, at which the amplitude is maximum, can be easily related to the phase lag of the $k\omega$ component of the response. The obtained amplitude and phase lag contain kinetic information of the system, and the dynamic behavior can be studied.

2.2. Transfer function and sinusoidal-wave stimulation

Transfer function is a convenient model to analyze frequency responses of a system [11]. In the Laplace-domain, the output response $Y(s)$ of a linear system can be conveniently related to an input function $U(s)$, i.e., stimulation, by the transfer function of the system $G(s)$

$$Y(s) = G(s) \cdot U(s) \tag{2}$$

When a sinusoidal-wave $u(t) = A \sin \omega t$ is applied as a stimulation function, the response of a system $Y(s)$ can be written as

$$Y(s) = G(s) \cdot A \frac{\omega}{s^2 + \omega^2} \tag{3}$$

Since in the Laplace-domain the sinusoidal-wave is,

$$\mathcal{L}(u(t)) = A \frac{\omega}{s^2 + \omega^2} \tag{4}$$

Expanding Eq. (3) into partial fractions, assuming that the poles of $G(s)$ are negative as in stable systems, and taking the inverse Laplace transform result in the following time-domain output $y(t)$ at steady-state:

$$y(t) = A|G(i\omega)| \sin(\omega t + \varphi) \tag{5}$$

where $|G(i\omega)|$ is the modulus and φ is the argument of $G(i\omega)$ ($\varphi = \measuredangle G(i\omega)$). Comparing the output function $y(t)$ with the input function $u(t)$, reveals that the output function has changes in the amplitude and the phase. The changes, the amplitude ratio (AR) and phase lag (PL), are simply written as follows:

$$AR = \frac{A|G(i\omega)|}{A} = |G(i\omega)|, \quad PL = \varphi = \measuredangle G(i\omega) \tag{6}$$

Eq. (6) allows calculating with ease the frequency response, i.e., the amplitude and phase change, when sinusoidal-wave stimulation is used.

When the time-domain output (Eq. (5)) is demodulated (Eq. (1)) at the fundamental frequency ($k = 1$, when $k \neq 1$ the demodulated response will be zero for a linear system), the following phase-domain signal is obtained

$$A(\phi^{PSD}) = A|G(i\omega)| \cos(\varphi - \phi^{PSD}) \tag{7}$$

2.3. Square-wave stimulation

The time-domain response to a square-wave stimulation can be analogously calculated as the response to the sinusoidal-wave stimulation. According to the well-known Fourier decomposition, a square-wave (SW) of amplitude A is written as the sum of sinusoidal waves of odd frequencies

$$SW = \frac{4}{\pi} A \left(\sin \omega t + \frac{1}{3} \sin 3\omega t + \frac{1}{5} \sin 5\omega t + \cdots \right)$$
$$= \frac{4}{\pi} A \sum_{n=1}^{\infty} \frac{1}{2n-1} \sin[(2n-1)\omega t] \tag{8}$$

In the Laplace-domain the square-wave is,

$$\mathscr{L}(SW(t)) = \frac{4}{\pi} A \sum_{n=1}^{\infty} \frac{\omega}{s^2 + [(2n-1)\omega]^2} \qquad (9)$$

Therefore, the response of a system $Y(s)$ can be written with a transfer function $G(s)$ as,

$$Y(s) = G(s) \cdot \frac{4}{\pi} A \sum_{n=1}^{\infty} \frac{\omega}{s^2 + [(2n-1)\omega]^2} \qquad (10)$$

Expanding Eq. (10) into partial fractions, assuming that the poles of $G(s)$ are negative as in stable systems, and taking the inverse Laplace transform results in the following time-domain output $y(t)$ at steady-state:

$$y(t) = \frac{4}{\pi} A \sum_{n=1}^{\infty} \left[\frac{1}{2n-1} |G(i(2n-1)\omega)| \sin((2n-1)\omega t + \varphi_{2n-1}) \right] \qquad (11)$$

where $|G(i(2n-1)\omega)|$ is the modulus and φ_{2n-1} is the argument of $G(i(2n-1)\omega)$. Clearly from Eqs. (8) and (11), the amplitude ratio and the phase lag of the $(2n-1)\omega$ frequency component between the input and the output functions can be expressed as,

$$AR_{2n-1} = |G(i(2n-1)\omega)|, \quad PL_{2n-1} = \varphi_{2n-1} = G(i(2n-1)\omega) \qquad (12)$$

When the time-domain output (Eq. (11)) is demodulated (Eq. (1)) at a $(2n-1)\omega$ frequency, the following phase-domain signal is obtained:

$$A_{2n-1}(\phi_{2n-1}^{PSD}) = \frac{4}{\pi} \frac{A}{2n-1} |G(i(2n-1)\omega)| \cos(\varphi_{2n-1} - \phi_{2n-1}^{PSD}) \qquad (13)$$

2.4. Relation between responses to sinusoidal- and square-wave stimulations

When the responses to sinusoidal- and square-wave simulations of the same amplitude are compared (Eqs. (7) and (13)), the amplitude and the phase lag of the responses are associated by the following relations:

$$A^{\sin}|_{1\omega'=(2n-1)\omega} = \frac{\pi}{4}(2n-1)A_{2n-1}^{SW} \qquad (14)$$

$$\varphi^{\sin}|_{1\omega'=(2n-1)\omega} = \varphi_{2n-1}^{SW} \qquad (15)$$

where $A^{\sin}|_{1\omega'=(2n-1)\omega}$ and $\varphi^{\sin}|_{1\omega'=(2n-1)\omega}$ are the amplitude and the phase lag of the phase-domain response to sinusoidal-wave stimulation when the fundamental frequency of the stimulation is equal to $(2n-1)\omega$, and A_{2n-1}^{SW} and φ_{2n-1}^{SW} are the amplitude and the phase lag of the phase-domain response to square-wave stimulation (stimulation frequency ω) obtained by the demodulation with the index $k = 2n - 1$. Neglecting the factor $\pi/4$, Eq. (14) shows that the demodulated response amplitude obtained with sinusoidal-wave stimulation at the $(2n-1)\omega$ modulation frequency is simply equal to the one obtained by square-

wave stimulation multiplied by the demodulation index $2n - 1$. Also, Eq. (15) shows that the phase lag of the response obtained by square-wave stimulation and demodulation at $(2n-1)\omega$ frequency is equal to the one obtained by sinusoidal-wave stimulation at the $(2n-1)\omega$ modulation frequency and demodulated at the fundamental frequency. The relations are intuitively reasonable when a linear system is considered and all the different frequency terms of a square-wave (Eq. (8)) can be treated separately. The main advantage of the relations in Eqs. (14) and (15) is the capability to obtain amplitudes and phase lags of higher frequencies from a single square-wave experiment. In other words, kinetic information usually obtained by a number of experiments with sinusoidal-wave stimulations at $1\omega, 3\omega, 5\omega, \ldots$ are acquired by a single experiment with a square-wave stimulation at 1ω. There is an upper limit for the demodulation frequency because the amplitudes of higher frequency terms in a square-wave decrease by the factor $2n - 1$ as seen in Eq. (8). The limit depends on the signal-to-noise ratio of responses. The better the signal-to-noise ratio is, the higher is the frequency term that can be used confidently in kinetic analysis.

3. Experimental methods

A small-volume cell specially designed for modulation excitation PM-IRRAS, built with the aim of fast gas exchange, was used to study the gas mixing property within the cell. The detailed description of the cell can be found elsewhere [10]. The flow characteristics and residence time distribution in the cell are reported in the *supporting material*. A schematic drawing and cross-section at the plane of light path of the setup are shown in Fig. 1. Briefly, the cell has an inner volume of ca. 6.9 mL, the light path length within the cell is 25.9 mm, and the length between the gas inlet and the sample surface is 7 mm. The gas inlet consists of five holes (each 0.7 mm diameter) targeting at the four edges of the sample and the center to allow fast gas exchange near the sample surface. The gas phase absorbance spectra were measured utilizing the sum-reflectivity of parallel and perpendicular polarized light, which is normally used for the compensation of gas phase absorbance upon obtaining the PM-IRRA surface spectra. When the absorbance of surface species is weak, the sum-reflectivity can simply be considered as a single beam spectrum of the gas phase.

An aluminum plate $(10 \times 10 \times 1\text{ mm})$ was mounted in the cell located within the compartment of a Bruker PMA 37 accessory, connected to an external beam port of a Bruker Vector 33 Fourier transform infrared spectrometer. The angle of incidence was 80°. CO (0.5 vol%) in Ar (PANGAS) and He (5.0, >99.999 vol%, PANGAS) were alternatively flowed into the cell at 20, 40, and 60 mL/min under atmospheric pressure at room temperature. CO (0.5%) and pure He were fed in the 1st and the 2nd half-period, respectively. Sixty spectra were recorded per modulation period. Signal averaging was performed
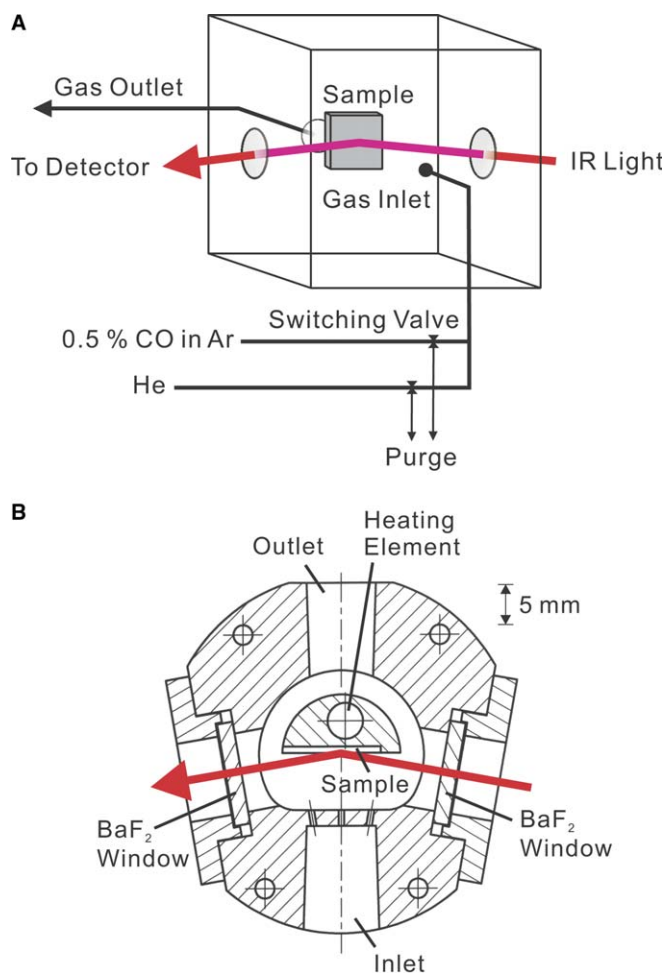
Fig. 1. (A) Schematic drawing of the experimental setup. (B) Cross-section of the ME PM-IRRAS cell at the plane of incident light. The light path is shown as red line with arrow.

over 20, 10, 5, 3 periods after 4, 2, 1, 1 initial periods which are necessary to reach quasi-steady-states with the modulation periods of 64.2, 128.8, 257.9, and 516.1 s, respectively. The last spectrum within the modulation period served as the reference to calculate absorbance spectra. CO gas concentration was calculated by integrating the absorbance of the CO stretching vibrational mode.

4. Model

In order to reasonably model the mixing behavior and also to consider the gas line volume before the gas inlet of the cell, a mixing tank with time delay model was used. The concentration change of a species in the tank can be described by a first order differential equation with a dead-time resulting in the following equation:

$$\tau \frac{dC}{dt} + C = C_{in}(t - \theta) \tag{16}$$

where C is the concentration in the tank, C_{in} is the inlet concentration, and θ and τ are the capacitive time con-

stant of the gas line and the cell, respectively. With the cell volume V_{cell}, the line volume V_{line}, and the volumetric flow rate of gas φ_V, θ and τ can be written as:

$$\theta = \frac{V_{line}}{\varphi_V}, \quad \tau = \frac{V_{cell}}{\varphi_V} \tag{17}$$

Hence, the differential equation (16) can be expressed as the following transfer function [12]:

$$G(s) = \frac{e^{-\theta s}}{\tau s + 1} \tag{18}$$

The errors between experimental data and data obtained by the model were first squared and summed up over the 12 different experiments (3 flow rates × 4 modulation frequencies) to obtain the overall SSE (sum of squared error) between experimental and theoretical data. The optimum cell volume V_{cell} and the optimum line volume V_{line} were determined by minimizing the SSE.

5. Results and discussion

Experimental responses at different flow rates and modulation frequencies are shown in Fig. 2 (solid lines). Clearly, more delay in the responses was observed at higher modulation frequencies and lower flow rate. The minimization of the SSE by varying V_{cell} and V_{line} yielded the optimum cell volume $V_{cell} = 7.164$ mL, and the optimum line volume $V_{line} = 2.246$ mL. Using these values and the model (Eq. (18)) the theoretical responses are computed and shown in Fig. 2 (dotted line). The agreement between the experimental and the theoretical responses was excellent. The optimum cell volume was in good agreement with the actual cell volume of ca. 6.9 mL.

Furthermore, the frequency response of the mixing behavior was analyzed by means of a Bode diagram. Upon constructing the Bode diagram, the relations in Eq. (14) were applied to obtain responses at frequencies up to 5ω for a square-wave modulation at 1ω. Fig. 3 shows the Bode diagram of both experimental and theoretical responses, and the values demodulated at different frequencies are shown as different symbol types (filled, half-filled, and empty). The different symbols (filled, half-filled, and empty) fit almost perfectly to the same curve for the amplitude ratios and reasonably well for the phase lags. The demodulated data points for the amplitude ratios (1, 3 and 5ω) do hardly show any scattering, whereas the corresponding data points for the phase lags are slightly scattered. This is a clear indication of a linear response of the system. In theory, such linear responses can occur when a system is intrinsically linear or a non-linear system is only slightly perturbed by a small stimulation. When a gas flow with more than one order of magnitude higher CO concentration (5–15% CO) was used for the modulation experiments, data demodulated at different frequencies deviated significantly from one single curve, particularly for the phase lags (see Supporting Material). This observation supports the
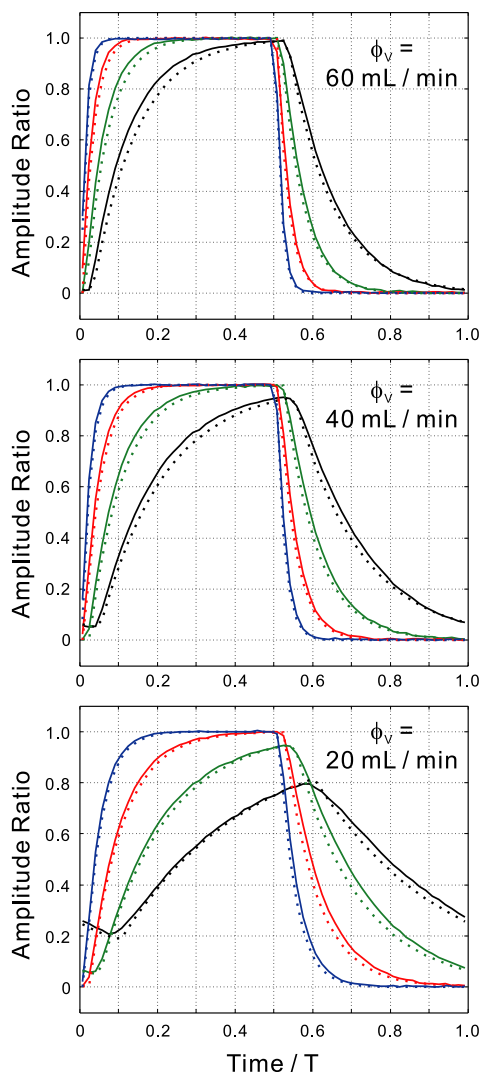
Fig. 2. Response comparisons between experiments (solid line) and simulations of the mixing tank model (dotted line) at 60, 40, and 20 mL/min. The blue, red, green, and black lines correspond to the modulation periods of 516.1, 257.9, 128.8 and 64.2 s, respectively. Time is shown relative to the modulation periods. $V_{cell} = 7.164$ mL and $V_{line} = 2.246$ mL were used for the simulations.
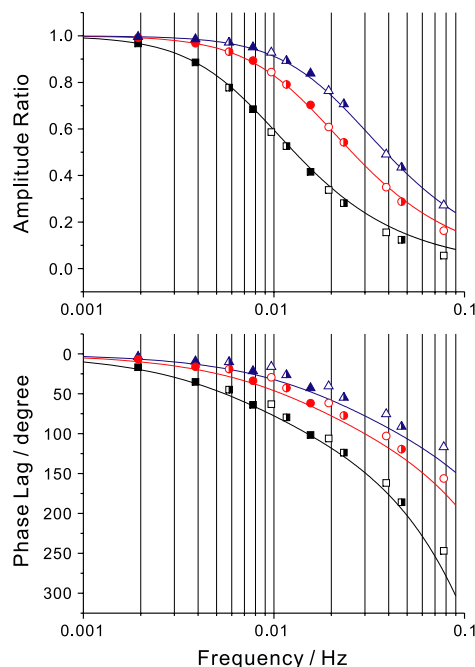

Fig. 3. Bode diagram of experimental data (symbols) and the mixing tank model (lines) at 60 mL/min (blue), 40 mL/min (red), and 20 mL/min (black). Square-wave concentration stimulations at 1.9, 3.9, 7.8, and 15.6 mHz (fundamental frequency) were used. The filled, the half-filled, and the empty symbols are the data demodulated at 1, 3, and 5ω, respectively. $V_{cell} = 7.164$ mL and $V_{line} = 2.246$ mL were used for the simulations.

latter possibility, i.e., a non-linear system behaving linearly due to the small stimulation (0.5% CO). Theoretical frequency responses were calculated using the optimum volumes and are shown in Fig. 3. The agreement between the experimental and theoretical frequency responses was excellent for the amplitude ratios and reasonable for the phase lags. The overall good agreement of the frequency responses suggests that the simple linear mixing tank with time delay model, is close to the linearized model of the actual very complex non-linear model. The linearity can also be promoted by the small perturbation, i.e., the small amplitudes of the higher frequency terms of the square-wave.

A practical importance of such simple models is their better comprehension due to the possibility to extract physically meaningful parameters. Complex models often suffer from too many fitting parameters and the difficulty to gain physical insights into a system. In order to study exactly the mixing property of the current cell, at least diffusion of gases and fluid dynamics have to be taken into account. This study gives effective cell and line volumes, which include all the effects of the system and are the easily understandable physical parameters, and the model is easily extendable to include other parameters such as chemical reactions.

One of the most important aspects of square-wave stimulation is the experimental easiness for its generation compared to exact sinusoidal-wave stimulation, especially when concentration is chosen as a perturbation parameter. Indeed, almost all the recent MES works rely on square-wave stimulation. This work will surely help to understand the outcome of demodulated data and how to make use of all the information contained in the phase-domain responses to a square-wave stimulation. Furthermore, the combination of square-wave stimulation and demodulation at fundamental and higher frequencies allow studying responses in a wide frequency range. It also allows studying frequency responses at experimentally non-feasible high frequencies. The non-linearity of most real systems will make it very difficult to determine the frequency responses exactly, however, when a sufficiently small stimulation is used and a number of modulation cycles are averaged to enhance signal-to-noise ratio and obtain higher frequency

terms of the response with high accuracy, the high frequency demodulation will serve as a good estimate of the responses at high frequencies. This can become very powerful in disentangling overlapping bands in a broadband spectrum, e.g., infrared-spectrum of several species. When overlapping bands, more precisely the species causing the bands, have different kinetics and the assignments of the bands are desired, for a MES experiment the modulation frequency should be chosen to maximize the phase difference, i.e., the kinetic behavior, of each band (an example is provided in the supporting material). Similar time-domain response of two signals may produce very different phase delay and amplitude ratio at high-frequency demodulation, and such a difference becomes clear by response-screening with demodulations at various frequencies.

6. Conclusion

The advantages and practical usefulness of square-wave stimulation in modulation excitation spectroscopy (MES) were shown. The response of a system to square-wave stimulation could be understood in terms of sinusoidal-waves constituting the stimulation. The response to square-wave stimulation was related to the one of sinusoidal-wave stimulation using a linear system model and, in particular, transfer function of a general system. The application example of the square-wave stimulation to investigate the gas-mixing property in a PM-IRRAS flow-through cell clearly demonstrated the usage of the relation. Sufficiently small stimulation amplitude is required to fully appreciate the relation derived in this study within the linear-response framework; however, high-frequency demodulation will serve as a practical tool to roughly estimate the amplitude and the phase delay to separate overlapping signals when a broadband detection technique is used. This work will be of practical use and help analyzing the responses to square-wave stimulation in MES.

Appendix A. Supplementary data

Residence time distribution in the PM-IRRAS cell, effect of tracer concentration on linear response behavior, and application of high frequency demodulation ($k = 3, 5, 7, \ldots, \omega$) in estimating kinetic parameters in broadband spectroscopy. Supplementary data associated with this article can be found, in the online version, at doi:10.1016/j.chemphys.2005.12.009.

References

[1] D. Baurecht, U.P. Fringeli, Rev. Sci. Instrum. 72 (2001) 3782.
[2] U.P. Fringeli, D. Baurecht, H.H. Günthard, in: H.U. Gremlich, B. Yan (Eds.), Infrared and Raman Spectroscopy of Biological Materials, Dekker, New York/Basel, 2000, p. 143.
[3] T. Bürgi, A. Baiker, J. Phys. Chem. B 106 (2002) 10649.
[4] I. Noda, Vib. Spectrosc. 36 (2004) 143.
[5] D. Baurecht, I. Porth, U.P. Fringeli, Vib. Spectrosc. 30 (2002) 85.
[6] M. Bieri, T. Bürgi, J. Phys. Chem. B 109 (2005) 10243.
[7] R. Wirz, T. Bürgi, A. Baiker, Langmuir 19 (2003) 785.
[8] R. Wirz, T. Bürgi, W. Lindner, A. Baiker, Anal. Chem. 76 (2004) 5319.
[9] A. Urakawa, R. Wirz, T. Bürgi, A. Baiker, J. Phys. Chem. B 107 (2003) 13061.
[10] A. Urakawa, T. Bürgi, H.-P. Schläpfer, A. Baiker, J. Chem. Phys. (in press).
[11] G. Stephanopoulos, Chemical Process Control, PTR Prentice Hall, New Jersey, 1984.
[12] B.W. Bequette, Process Dynamics, Prentice Hall PTR, New Jersey, 1998.